Electrochemical Polymerization of Fluoranthene and Characterization of Its Polymers

Jingkun Xu,*,† Jian Hou,†,‡ Shusheng Zhang,‡ Qiang Xiao,† Rui Zhang,§ Shouzhi Pu,† and Qingli Wei‡

Jiangxi Key Laboratory of Organic Chemistry, Jiangxi Science and Technology Normal University, Nanchang 330013, China, College of Chemistry and Molecular Engineering, Qingdao University of Science and Technology, Qingdao 266042, China, and NSF IUCR Center for Advanced Studies in Novel Surfactants, Langmuir Center for Colloids and Interfaces, Columbia University, 930 Mudd Building, New York, New York 10027

Received: October 7, 2005; In Final Form: December 20, 2005

A novel inherently conducting polymer, high-quality polyfluoranthene (PFA) film with electrical conductivity of 10^{-2} S cm^{-1}, was first synthesized electrochemically by direct anodic oxidation of fluoranthene in a middle strong Lewis acid—boron trifluoride diethyl etherate. The oxidation potential onset of fluoranthene in this medium was measured to be only 1.07 V vs SCE, which was much lower than that in acetonitrile + 0.1 mol L^{-1} tetrabutylammonium tetrafluoroborate (1.68 V vs SCE). This PFA film showed good redox activity and stability even in concentrated sulfuric acid. Moreover, the fluorescence properties of PFA were greatly improved in comparison with those of the monomer. Dedoped PFA films were partly soluble in polar solvents such as CH_2Cl_2, acetone, tetrahedrofuran, and dimethyl sulfoxide. The structure and morphology of the polymer were investigated by UV−vis spectroscopy, infrared spectroscopy, and scanning electron microscopy, respectively. The results of quantum chemistry calculations of fluoranthene monomer and ^{1}H NMR spectroscopy of dedoped PFA films indicated that the polymerization mainly occurred at $C_{(3)}$, $C_{(4)}$, $C_{(13)}$, and $C_{(14)}$ positions.

1. Introduction

Conjugated polymers, which possess properties of both organic polymers and inorganic conductors or semiconductors, have become the subject of intensive studies, owing to their most well-known ability—to conduct electrical current after being partially oxidized (p-doping) or reduced (n-doping). Their conductive ability is directly related to their delocalized π-system extending over a large number of repeat units.[1,2] Besides the conducting properties, the conjugated polymers also showed several other excellent properties such as optical and fluorescence properties which cater to the applications in optoelectronics. Therefore, the pursuit of high-quality polymer films is still one of the main goals in the research and development of inherently conducting polymers, due to their potential applications in rechargeable batteries, electrochromic display devices, supercapacitors, antistatic coating, and biosensors. The most attractive properties of conducting polymers were that their properties could be tuned by structural modification. Structural considerations therefore became an important factor to take into account in the synthesis of new materials.

Fluoranthene, constructed by linking a benzene group and a naphthalene group with two single C−C bonds, was often used as a dopant of molecular crystals for laser spectroscopy.[3] The fluoranthene molecules with the extended π-electron systems have attracted a considerable interest in the field of synthetic metals and a promising block for building high-quality conducting polymers.[4] Fluoranthene also has various anomalous fluorescence characteristics, i.e., long lifetime and high quantum yield in comparison with expected value from calculation, large Stokes' loss, immunity of concentration quenching and excimer formation, and the inertness to oxygen quenching.[5] As a polymer, polyfluoranthene (PFA) has potential interests for electroluminescence and photovoltaics. Moreover, the main point for the polymerization of fluoranthene may lie in the structural similarity between polyfluoranthene and polyfluorene, and the applications of the latter as well as its derivatives in light emitting dioxide meet their explosive academic reports during the past eight years. However, up to now, the polymerization of fluoranthene[6,7] and the structures and properties of PFA have been rarely studied. The reason probably results from the complicated conditions that were required for fluoranthene polymerization, for example, the high oxidation potential needed in common organic media such as acetonitrile during electrochemical polymerization process generally lead to the poor quality of conducting polymer films.

In recent years, boron trifluoride diethyl etherate (BFEE) was found to be a good electrolyte for electrochemical polymerization of aromatic compounds[8] such as pyrrole,[9,10] furan,[11,12] thiophene, benzene, naphthalene, anthracene,[13−20] indole and its derivatives,[21−25] selenophene,[26,27] etc. Utilizing BFEE, the oxidation potentials of aromatic monomers can be considerably lowered. Meanwhile, the mechanical properties and flexibility of the conducting polymers were greatly improved with the formation of long polymer chains.

In present work, pure BFEE was first applied for the electrochemical polymerization of fluoranthene. As a result, high-quality PFA films can be easily electrodeposited by direct anodic oxidation of fluoranthene. The electrochemical properties, spectroscopic properties, thermal stability, and morphology of

* To whom correspondence should be addressed. Tel: +86-791-3805183. Fax: +86-791-3826894. E-mail: xujingkun@tsinghua.org.cn or xujingkun@mail.ipc.ac.cn.

† Jiangxi Science and Technology Normal University.

‡ Qingdao University of Science and Technology.

§ Columbia University.

10.1021/jp055710b CCC: $33.50
Published on Web 01/21/2006

as-prepared PFA films, especially fluorescent properties together with polymerization mechanism were studied in detail.

2. Experimental Section

2.1. Reagents and Treatment. BFEE (Beijing Changyang Chemical Plant) was distilled and stored at −20 °C before use. Fluoranthene (Acros Organics) and commercial high-performance liquid chromatography grade acetonitrile (ACN, Tianjin Guangfu Fine Chemical Research Institute) were used directly without further purification. Tetrabutylammonium tetrafluoroborate (TBATFB, Acros Organics, 95%) was dried in a vacuum at 60 °C for 24 h before use. Deuterium substituted chloroform ($CDCl_3$) and 25% ammonia were made by Beijing Chemical Plant.

2.2. Apparatus. The conductivity of as-formed PFA film was measured by the conventional four-probe technique with pressed pellets of the samples. UV−visible spectra were taken by using a Perkin-Elmer Lamda 900 UV−vis−NIR spectrophotometer. The infrared (IR) spectra were recorded by using KBr pellets of the polymers on the Nicolet 510P FT-IR spectrometer. The fluorescence spectra were determined with an F-4500 fluorescence spectrophotometer (Hitachi). The ^1H NMR spectra were recorded on a Bruker AV 400 NMR spectrometer, and $CDCl_3$ was used as the solvent. The thermogravimetric (TG) and differential thermogravimetric (DTG) analyses were performed with a thermal analyzer of Netzsch TG209. Scanning electron microscopy (SEM) measurements were taken by using a JEOL JSM-6700F scanning electron microscope.

2.3. Electrosyntheses of Polymer Films. The electrochemical polymerizations and examinations were performed in a one-compartment cell by using a model 263 potentiostat−galvanostat (EG & G Princeton Applied Research). Platinum wires with surface areas of 0.2 and 0.4 cm^2 were used as the working and counter electrodes, respectively. According to previous reports,[15] two stainless steel sheets (AISI 304, 10 × 20 mm) placed 10 mm apart were used as the working (10 cm^2) and counter electrodes (12 cm^2). Before every polymerization, they were carefully polished with abrasive paper (1500 mesh) and cleaned with water and acetone successively and then dried by a blower. All potentials were referred to SCE.

The typical electrolytic solutions were distilled BFEE containing 50 mmol L^{-1} fluoranthene. All solutions were deaerated by a dry argon stream for 10 min before the experiment, and a slight argon overpressure was maintained during the experiment. PFA films were grown potentiostatically. Their thickness was controlled by the total charges through the cell, and the charge values were read directly from $j-E$ curves. After polymerization, PFA films were peeled off the electrode surfaces. Then they were washed repeatedly with acetone to remove the electrolyte and monomer. For spectral studies, PFA films were dedoped with 25% ammonia for 3 days and then washed repeatedly with distilled water and acetone. Finally, they were dried under vacuum at 60 °C for 24 h.

3. Results and Discussion

3.1. Electrochemical Syntheses of PFA Films. The anodic polarization curves of fluoranthene in pure BFEE and in ACN containing 0.1 mol L^{-1} TBATFB are shown in Figure 1. The oxidation onset of fluoranthene was initiated at 1.07 V vs SCE in pure BFEE, which was relatively lower than that of fluoranthene in ACN containing 0.1 mol L^{-1} TBATFB (1.68 V vs SCE). This indicated that the oxidation of fluoranthene in BFEE was much easier than that in ACN/TBATFB. The reason lies in that BFEE can interact with the aromatic ring of the monomer, which reduced the resonance stability of the aromatic ring through the formation of π-complexes between the monomer and BFEE, making electron loss from fluoranthene much easier. In consequence, the oxidation potential of fluoranthene in pure BFEE was reduced more sharply than that in ACN.

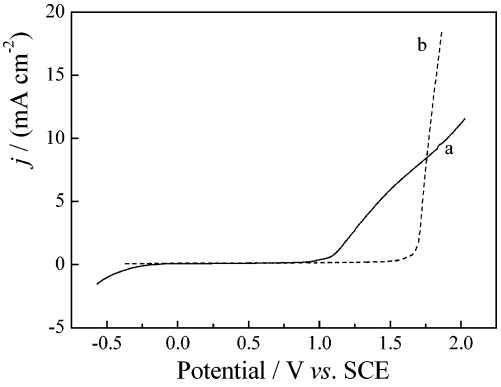

Figure 1. Anodic polarization curves of fluoranthene in pure BFEE (a) and in ACN + 0.1 mol L^{-1} TBATFB (b). Potential scan rates: 20 mV s^{-1}.

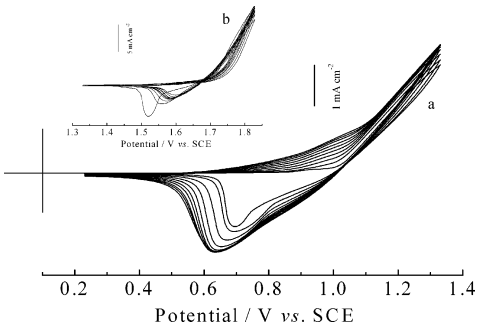

Figure 2. Cyclic voltammograms of 50 mmol L^{-1} fluoranthene in pure BFEE (a) and in ACN + 0.1 mol L^{-1} TBATFB (b). Potential scan rates: 100 mV s^{-1}.

The successive cyclic voltammograms (CVs) of 50 mmol L^{-1} fluoranthene in pure BFEE and ACN on Pt electrode are shown in parts a and b of Figure 2, respectively. The CVs of fluoranthere in pure BFEE (Figure 2a) showed characteristic features like other conducting polymers, such as polypyrrole and polythiophene. As the CV scan continues, the color of the solution close to the working electrode changed slightly from colorless to transparent red, then to opaque deep red, indicating that part of the monomer was oxidized into short-chain oligomers which were stable enough to dissolve or disperse in the solvent. Simultaneously, a thin and uniform polymer film was formed on the working electrode surface and could be taken out from the electrolytic solution after CVs. The redox peaks at 1.0 and 0.65 V were attributed to the p-doping/dedoping processes of the PFA film formed in previous potential scans. The increase of the redox current with increasing cycle number of the potential scans indicated that the amount of the polymer deposited on the electrode increased. The results indicated that PFA films deposited on Pt wire anode had good redox activity.

In comparison, the CVs of fluoranthene in ACN were not very satisfactory (Figure 2b). In addition, PFA films can also be prepared potentiostatically at 1.23 V vs SCE from BFEE. However, using the same method (constant applied potential 1.83 V vs SCE) only leads to form a trace amount of the polymer in ACN. This demonstrates that BFEE is the more suitable medium for the electrosyntheses of high-quality PFA films than ACN.

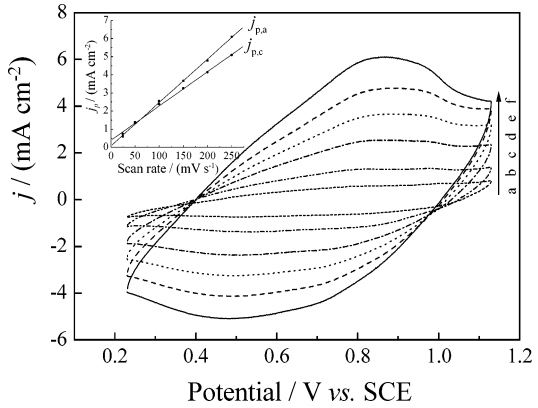

Figure 3. Cyclic voltammograms of PFA films in pure BFEE at potential scan rates of 25 mV s^{-1} (a), 50 mV s^{-1} (b), 100 mV s^{-1}(c), 150 mV s^{-1} (d), 200 mV s^{-1} (e), and 250 mV s^{-1}(f), respectively. The films were synthesized electrochemically in pure BFEE at a constant applied potential of 1.23 V vs SCE.

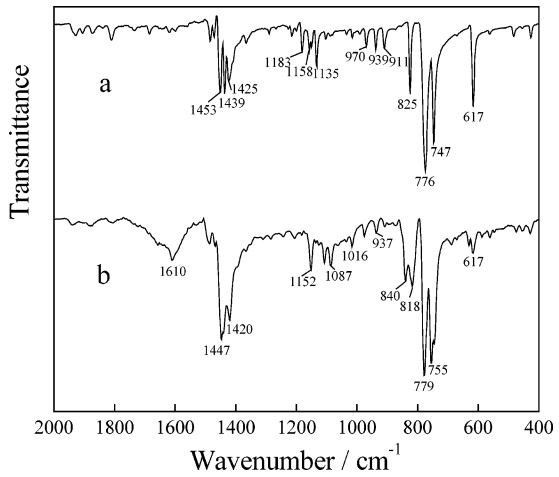

Figure 4. FTIR spectra of the fluoranthene monomer (a) and dedoped PFA films (b) obtained potentiostatically at 1.23 V vs SCE from pure BFEE after a treatment with 25% aqueous ammonia for 3 days.

3.2. Electrochemistry of PFA Films. The electrochemical behavior of PFA films from pure BFEE was studied in concentrated sulfuric acid (Figure 3). Similar to the results in the literature,[28] the steady-state cyclic voltammograms represented broad anodic and cathodic peaks. The peak current densities were proportional to the scan rates (inset of Figure 3), indicating good redox activity of the polymer. Furthermore, these films could be cycled repeatedly between the conducting (oxidized) and insulating (neutral) states without significant decomposition of the materials, indicating the high structure stability of the polymer even in concentrated sulfuric acid. The films from BFEE can be oxidized and reduced from 0.86 (E_a) to 0.47 V (E_c) in concentrated sulfuric acid. The difference of ($E_a - E_c$) related to the kinetics of the doping−dedoping reactions is equal to 0.39 in concentrated sulfuric acid for the PFA from BFEE. The broad redox waves in their CVs can be ascribed to the presence of coupling defects distributed statically, which results in a series of energetically nonequivalent chain segments.

3.3. Structural Characterizations. The strong and narrow peaks at 747 and 776 cm^{-1} in the IR spectrum of fluoranthene (Figure 4a), which are broader and shifted to 755 and 779 cm^{-1} in the spectrum of dedoped PFA film (Figure 4b), are owing to out-of-plane bending modes. Meantime, these modes also produce a substantial number of moderately strong bands in the 1500−1400 cm^{-1} range, such as 1425, 1439, and 1453 cm^{-1} in the monomer spectrum (Figure 4a) and 1420 and 1447 cm^{-1} in the polymer spectrum (Figure 4b), respectively.[29] The width and shift of peaks in the fluoranthene with the dedoped PFA film indicated that the electrochemical polymerization of fluoranthene occurred.

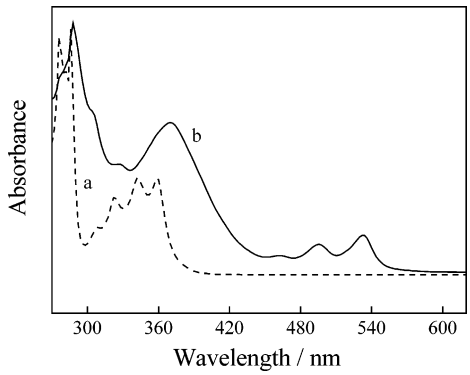

Figure 5. UV−vis spectra of fluoranthene (a) and dedoped PFA films (b) prepared from pure BFEE. Solvent: CH_2Cl_2.

The dedoped PFA films from BFEE can dissolve in polar organic solvents such as CH_2Cl_2, acetone, THF, DMSO, etc. The UV−vis spectra of fluoranthene and dedoped PFA dissolved in CH_2Cl_2 were examined, as shown in Figure 5. The fluoranthene monomer showed several characteristic absorptions at 276, 286, 323, 342, and 332 nm (Figure 5a). However, the spectra of the dedoped PFA films showed a much broader absorption with several absorptions at 288, 370, 496, and 533 nm. The overall absorption tailed off to about 600 nm (Figure 5b). Generally, the longer wavelength is the absorption, the higher conjugation length is the polymer.[30] Therefore, the results in Figure 5b indicated a longer polymer sequence was formed.

The fluorescence of dedoped PFA was examined using CH_2Cl_2 as the solvent using steady-state fluorescence spectroscopy in solution at room temperature through the 3-D scans of excitation−emission−intensity, as shown in Figure 6. The excitation−emission wavelength scans of fluoranthene (Figure 7a,b) and dedoped PFA in CH_2Cl_2 (2.0×10^{-4} g L^{-1}, Figure 7A,B) were also recorded. According to Figures 6 and 7, the fluoranthene monomer showed excitation spectra at 243, 288, 344, and 361 nm (Figure 7a), while the excitation spectra of PFA films had peaks at 250, 292, and 374 nm (Figures 6 and 7a). On the other hand, there were obvious peaks of excitation spectra found at 450 nm for the monomer (Figure 7b), while the relative intensity of the excitation spectra of the dedoped PFA films was even stronger with several peaks at around 496 and 533 nm (Figures 6 and 7B). According to Figure 7, the fluorescence intensity was very high with a low concentration of the fluoranthene and PFA films. Under the same conditions, the relative fluorescence intensity of dedoped PFA was obviously stronger and broader than that of fluoranthene monomer. This indicated that the fluorescence properties of PFA were greatly improved in comparison with those of the monomer. At the same time, the wide peak distribution can be ascribed to the wide molar mass distribution of PFA, in well accordance with UV−visible spectra.

To get deep insight into PFA structures and the polymerization mechanism, the atomic electron density population and reactivity of fluoranthene monomer (Scheme 1) were calculated at the B3LYP/6-31G (d,p) level using Hyperchem software. The results of main atomic electron density populations showed negative electric charges on $C_{(3)}$, $C_{(4)}$, $C_{(7)}$, $C_{(8)}$, $C_{(13)}$, and $C_{(14)}$ (Table 1), which implied that these atoms will donate electrons when the fluoranthene monomer is electrochemically polym-

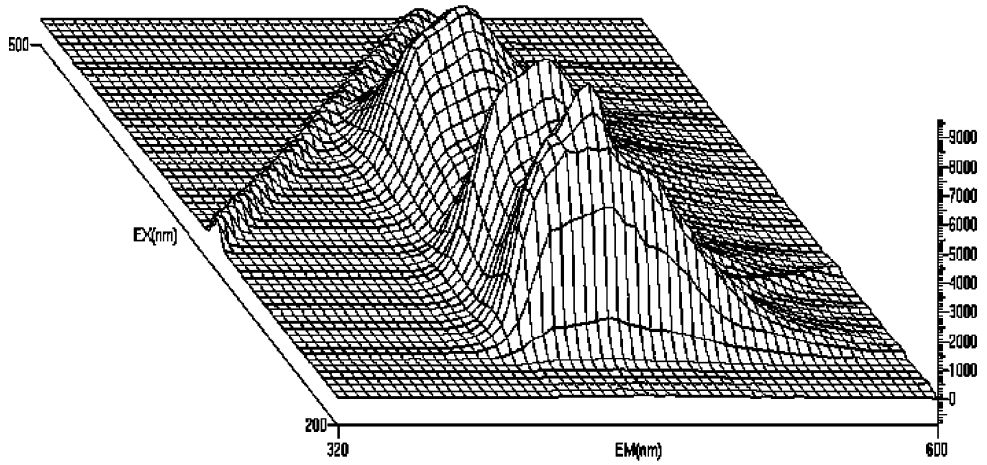

Figure 6. Three-dimensional fluorescence spectra of dedoped PFA prepared from BFEE. The *X* axis shows the emission wavelength, the *Y* axis shows the excitation wavelength, and the *Z* axis shows the relative intensity. Solvent: CH_2Cl_2. The concentration of the polymer was 2.0×10^{-4} g L^{-1}.

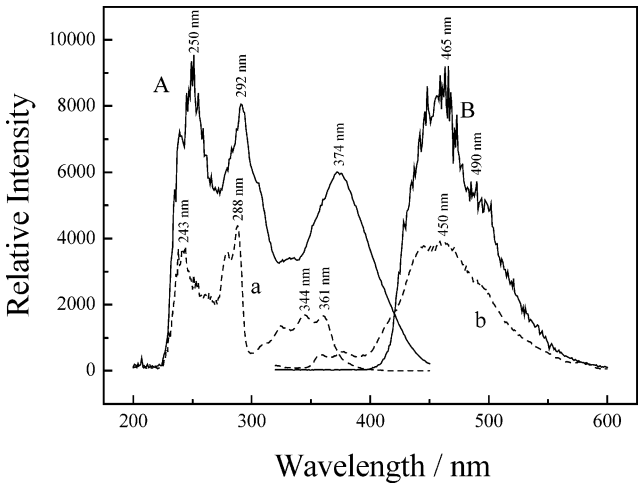

Figure 7. Emission (EM) and excitation (EX) spectra of fluoranthene (a, b) and dedoped PFA (A, B) prepared from BFEE. Solvent: CH_2Cl_2. The concentrations of the monomer and the polymer were both 2.0×10^{-4} g L^{-1}.

SCHEME 1: Structural Formula of Calculated Fluoranthene

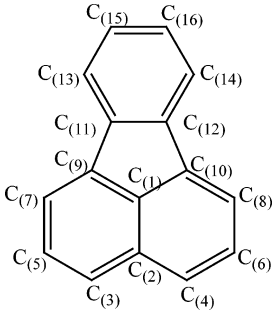

erized because the polymerization is performed through radical cation intermediates. According to the molecular orbital theory, the reaction between the active molecules mainly happens on the frontier molecular orbitals and near orbitals. For fluoranthene, the proportions of atoms $C_{(3)}$, $C_{(4)}$, $C_{(9)}$, $C_{(10)}$, $C_{(13)}$, and $C_{(14)}$ in HOMO were higher than other atoms as listed in Table 2. At the same time, $C_{(3)}$, $C_{(4)}$, $C_{(13)}$, and $C_{(14)}$ also had rich negative charges (Table 1). So, this implied that the polymerization between the monomer would happen preferentially on $C_{(3)}$, $C_{(4)}$, $C_{(13)}$, or $C_{(14)}$.

TABLE 1: Main Atomic Electron Density Populations for Fluoranthene

atom	electric charge	atom	electric charge
$C_{(1)}$	−0.078961	$C_{(2)}$	0.161015
$C_{(3)}$	−0.143703	$C_{(4)}$	−0.143694
$C_{(5)}$	−0.086099	$C_{(6)}$	−0.086098
$C_{(7)}$	−0.155431	$C_{(8)}$	−0.155447
$C_{(9)}$	0.093807	$C_{(10)}$	0.093829
$C_{(11)}$	0.043136	$C_{(12)}$	0.043126
$C_{(13)}$	−0.131729	$C_{(14)}$	−0.131725
$C_{(15)}$	−0.092015	$C_{(16)}$	−0.092015

TABLE 2: Main Composition and Proportion of the Frontier Orbitals in Fluoranthene (%)

atom	HOMO − 1	HOMO	LUMO	LUMO + 1
$C_{(1)}$	15.9299	0.0266	0.0265	1.0073
$C_{(2)}$	0.0523	0.0358	0.0448	13.3219
$C_{(3)}$	4.8196	13.0625	13.7535	1.6704
$C_{(4)}$	4.8201	13.0612	13.7535	1.6699
$C_{(5)}$	2.1135	4.9897	3.3901	4.7746
$C_{(6)}$	2.1135	4.9905	3.3904	4.7748
$C_{(7)}$	1.1249	6.8411	10.2433	11.1311
$C_{(8)}$	1.1253	6.8401	10.2443	11.1302
$C_{(9)}$	3.2204	11.5322	9.8104	1.2644
$C_{(10)}$	3.2207	11.5314	9.8109	1.2642
$C_{(11)}$	16.5101	0.0817	6.6287	2.4934
$C_{(12)}$	16.5101	0.0817	6.6291	2.4939
$C_{(13)}$	0.9075	9.8112	1.1529	16.6905
$C_{(14)}$	0.9077	9.8112	1.1531	16.6898
$C_{(15)}$	13.3130	3.6513	4.9844	4.8121
$C_{(16)}$	13.3117	3.6521	4.9840	4.8115

To further explore the polymer structure and the polymerization mechanism of fluoranthene, the ^{1}H NMR spectra of fluoranthene (Figure 8a) and the dedoped PFA obtained from pure BFEE were recorded (Figure 8b). The ^{1}H chemical shifts, according to the literature,[31] of fluoranthene are listed in Table 3. There were five group peaks as shown in Figure 8a. However, after polymerization, some new peaks appear and most of the peaks move to lower field. Generally, with introducing longer conjugation length into the polymer main backbone, the chemical shift of hydrogen atom on the aromatic rings usually moves to lower fields. Therefore, the phenomena in Figure 8a can be ascribed to the introduction of higher conjugation length in the PFA main chain.[32] The ^{1}H NMR data of PFA are assigned, as listed in Table 3. From Table 3 and Figure 8, it can be clearly seen that the coupling sites of the monomer units was very complicated. The proposed coupling mechanism of fluoranthene

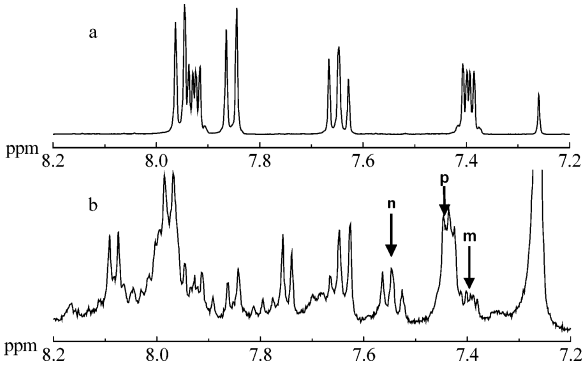

Figure 8. ^{1}H NMR spectra of fluoranthene (a) and dedoped PFA prepared from pure BFEE (b). Solvent: $CDCl_3$.

TABLE 3: ^{1}H NMR Data of δ_H for Fluoranthene Monomer and PFA

atom	C_3, C_4	C_5, C_6	C_7, C_8	C_{13}, C_{14}	C_{15}, C_{16}
fluoranthene	7.86	7.66	7.96	7.93	7.40
PFA	7.86, 7.9−8.0	7.66, 7.7−7.8	7.9−8.0	8.07	7.45, 7.5−7.6

SCHEME 2: Possible Mechanism for the Polymerization of Fluoranthene

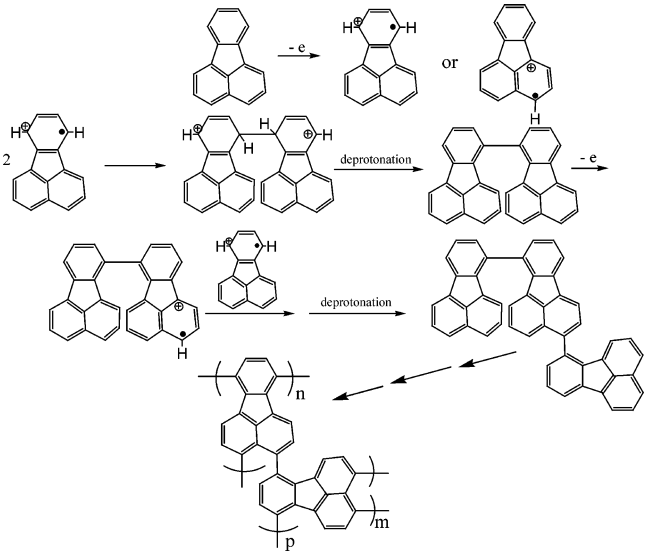

is illustrated in Scheme 2. There were three main coupling sites groups. The first one was $C_{(13)}$ and $C_{(14)}$ (coupling **n** in Scheme 2). The second one was $C_{(3)}$ and $C_{(4)}$ (coupling **m** in Scheme 2). The last one was $C_{(3)}$ or $C_{(4)}$ and $C_{(13)}$ or $C_{(14)}$ (coupling **p** in Scheme 2). The three-polymerization mechanism coexisted in as-formed PFA films, which were strongly supported by the computational results and the ^{1}H NMR spectra of the polymer. For example, the proton chemical shift from 7.4 to 7.6 can be ascribed to the protons at $C_{(15)}$ and $C_{(16)}$ (Figure 8). There were three main peaks in this region of the spectrum of PFA (Figure 8b). The peaks at ca. 7.55 can be assigned to the coupling **n** through $C_{(13)}$ and $C_{(14)}$ positions. Under this circumstance, the conjugation through $C_{(15)}$ and $C_{(16)}$ was extended after polymerization. This made the chemical shift of the protons on $C_{(15)}$ and $C_{(16)}$ move to lower field. On the other hand, the proton chemical shift on $C_{(15)}$ and $C_{(16)}$, at ca. 7.40, was almost stable during coupling **m** through $C_{(3)}$ and $C_{(4)}$, in comparison with those of the monomer (Figure 8). Meanwhile, the coupling **p** through $C_{(3)}$ or $C_{(4)}$ and $C_{(13)}$ or $C_{(14)}$, with the moderate extension of the conjugation length of the polymer, made the chemical shift of $C_{(15)}$ and $C_{(16)}$ to about ca. 7.43.

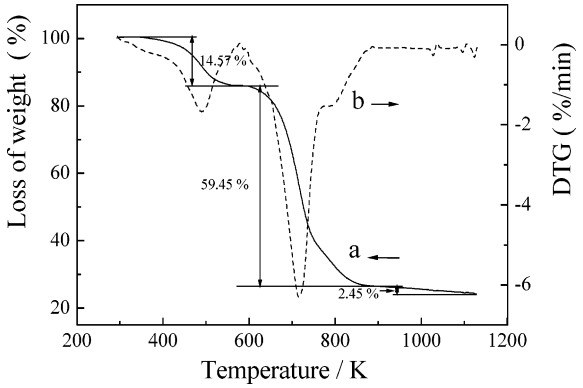

Figure 9. TGA curves of dedoped PFA films obtained potentiostatically at 1.23 V vs SCE from BFEE after a treatment with 25% aqueous ammonia for 3 days.

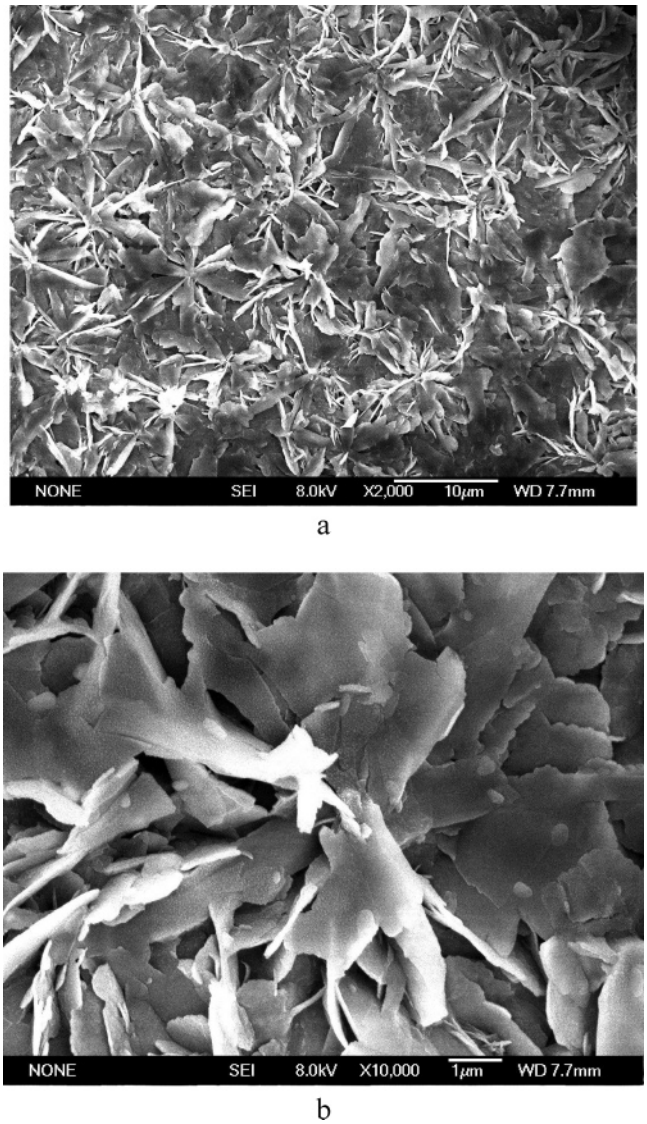

Figure 10. SEM micrographs of a PFA film deposited on the electrode surface from pure BFEE at a constant applied potential of 1.23 V vs SCE.

In comparison with the other two coupling mechanisms of **n** and **m** by integrating the peak areas, the coupling mechanism **p** dominated through the polymerization. The proton chemical shift of $C_{(5)}$ and $C_{(6)}$ also supported the three-polymerization mechanism. Therefore, it can be reasonably concluded that the

polymerization of fluoranthene was formed through the $C_{(3)}$, $C_{(4)}$, $C_{(13)}$, or $C_{(14)}$ position.

3.4. Thermal Analysis. The thermal analysis was performed under a nitrogen stream from 293 to 1128 K with a heating rate of 10 K/min (Figure 9). The structure of the main PFA backbone chain was kept up to 560 K. There was three-step loss of weight (Figure 9a). The first one is from 293 to 560 K, up to 14.57%, which can be ascribed to water evaporation or other moisture trapped in the polymer.[33] The second one occurred from 560 to 890 K, up to 59.45%, which was attributed to the degradation of the skeletal PFA backbone chain structure. The last one was about 2.45% from 890 to 1128 K, possibly owing to the overflow of some oligmers that decomposed from the PFA. From the DTG curves (Figure 9b), the fastest weight change rate of PFA films occurred at 715 K.

3.5. Morphology and Conductivity. The typical SEM images of PFA films are shown in Figure 10. Macroscopically, PFA films were flat and compact. Microscopically, the polymer films grew as irregular nano-sheets (200 nm or so) and resembled a growth of aggregates shaped as blossoms. The morphology with large void facilitates the movement of doping anions in to and out of the polymer film during doping and dedoping process, in well accordance with the higher redox activity of PFA films in concentrated sulfuric acid (Figure 3). This is also very interesting because conducting polymer films prepared from BFEE were generally flat, compact, and dense. The formation of PFA nano-sheets indicated that the polymer itself acted as a template during the polymerization. This also confirmed the better properties of PFA from BFEE than that of ACN. The conductivity of the PFA film from BFEE was measured to be 10^{-2} S cm^{-1}.

4. Conclusion

For the first time, high-quality PFA films, with good electrochemical properties, thermal stability (up to 560 K), and good optical properties, were electrochemically synthesized in pure BFEE by direct anodic oxidation of fluoranthene. The oxidation potential of fluoranthene in pure BFEE was determined to be only 1.07 V, which was lower than that in ACN + 0.1 mol L^{-1} TBATFB, 1.68 V. As-formed PFA films from pure BFEE showed good redox activity and high electrochemical stability in concentrated sulfuric acid. Quantum chemistry calculations and ^{1}H NMR spectra showed that the polymer chains were grown mainly via the coupling of the monomer at $C_{(3)}$, $C_{(4)}$, $C_{(13)}$, $C_{(14)}$ positions. PFA itself can assemble into nano-sheets (200 nm or so).

Acknowledgment. The Natural Science Foundation of Jiangxi Province (No. 050017 and No. 20564001), Nanchang University Testing Fund (2005013), and Jiangxi Science and Technology Normal University are acknowledged for their financial support.

References and Notes

(1) *Handbook of conducting polymers*; Skotheim, T. A., Ed.; Marcel Dekker: New York, 1986.
(2) *Handbook of conducting polymers*, 2nd ed.; Skotheim, T. A., Elsembaumer, R. L., Reynolds, J. R., Eds.; Marcel Dekker: New York, 1998.
(3) Marciniak, B. *J. Cryst. Growth.* **2002**, *236*, 333.
(4) Sachs, G.; Dormann, E. *Synth. Met.* **1988**, *25*, 157.
(5) Bark, K. M.; Force, R. K. *Spectrochim. Acta A* **1993**, *49*, 1605.
(6) Rubio, M.; Sanchezmarin, J.; Orti, E. *Synth. Met.* **1995**, *71*, 2081.
(7) Kertesz, M.; Ashertehrani, A. *Macromolecules* **1996**, *29*, 940.
(8) Chen, W.; Xue, G. *Prog. Polym. Sci.* **2005**, 783.
(9) Xu, J. K.; Shi, G. Q.; Qu, L. T.; Zhang, J. X. *Synth. Met.* **2003**, *136*, 221.
(10) Wan, X. B.; Liu, X.; Xue, G.; Jiang, L. X.; Hao, J. J. *Polymer* **1999**, *40*, 4907.
(11) Liu, C.; Zhang, J. X.; Shi, G. Q.; Zhao, Y. F. *J. Phys. Chem. B* **2004**, *108*, 2195.
(12) Wan, X. B.; Yan, F.; Jin, S.; Liu, X. R.; Xue, G. *Chem. Mater.* **1999**, *11*, 2400.
(13) Shi, G. Q.; Jin, S.; Xue, G.; Li, C. *Science* **1995**, *267*, 994.
(14) Shi, G. Q.; Li, C.; Liang, Y. Q. *Adv. Mater.* **1999**, *11*, 1145.
(15) Shi, G. Q.; Xue, G.; Li, C.; Jin, S. *Polym. Bull.* **1994**, *33*, 325.
(16) Li, C.; Shi, G. Q.; Liang, Y. Q. *J. Electroanal. Chem.* **1998**, *455*, 1.
(17) Huang, Z. M.; Qu, L. T.; Shi, G. Q.; Chen, F. E.; Hong, X. Y. *J. Electroanal. Chem.* **2003**, *556*, 159.
(18) Li, C.; Shi, G. Q.; Liang, Y. Q.; Ye, W.; Sha, Z. L. *Polymer* **1997**, *38*, 5023.
(19) Wang, X. F.; Shi, G. Q.; Liang, Y. Q. *Electrochem. Comm.* **1999**, *1*, 536.
(20) Fan, B.; Qu, L. T.; Shi, G. Q. *J. Electroanal. Chem.* **2005**, *575*, 287.
(21) Xu, J. K.; Nie, G. M.; Zhang, S. S.; Han, X. J.; Hou, J.; Pu, S. Z. *J. Polym. Sci. A: Polym. Chem.* **2005**, *43*, 1444.
(22) Xu, J. K.; Zhou, W. Q.; Hou, J.; Pu, S. Z.; Yan, L. S.; Wang, J. W. *J. Polym. Sci. A: Polym. Chem.* **2005**, *43*, 3986.
(23) Xu, J. K.; Zhou, W. Q.; Hou, J.; Pu, S. Z.; Yan, L. S.; Wang, J. W. *Mater. Lett.* **2005**, *59*, 2412.
(24) Xu, J. K.; Zhou, W. Q.; Hou, J.; Pu, S. Z.; Yan, L. S.; Wang, J. W. *Chin. J. Polym. Sci.* In press.
(25) Xu, J. K.; Wei, Z. H.; Hou, J.; Pu, S. Z. *Acta Polym. Sin.* In press.
(26) Pu, S. Z.; Hou, J.; Xu, J. K.; Nie, G. M.; Zhang, S. S.; Shen, L.; Xiao, Q. *Mater. Lett.* **2005**, *59*, 1061.
(27) Xu, J. K.; Hou, J.; Zhang, S. S.; Nie, G. M.; Pu, S. Z.; Shen, L.; Xiao, Q. *J. Electroanal. Chem.* **2005**, *578*, 345.
(28) Pandey, P. C.; Prakash, R. *J. Electrochem. Soc.* **1998**, *145*, 4103.
(29) Oomens, J.; Meijer, G.; Helden, von G. *J. Phys. Chem. A* **2001**, *105*, 8302.
(30) Sak-Bosnar, M.; Budimir, M.; Kovač, S.; Kukulj, D.; Duĭc, L. *J. Polym. Sci. Part A: Polym. Chem.* **1992**, *30*, 1609.
(31) Lutnaes, B. F.; Luthe, G.; Brinkman, U. A. T.; Johansen, J. E.; Krane, J. *Magn. Reson. Chem.* **2005**, *43*, 588.
(32) Xu, J. K.; Hou, J.; Zhou, W. Q.; Nie, G. M.; Pu, S. Z.; Zhang, S. S. *Spectrochim. Acta A* In press.
(33) Thieblemont, J. C.; Brun, A.; Marty, J.; Planche, M. F.; Calo, P. *Polymer* **1995**, *36*, 1605.